

Electronic Supplementary Information for

Smart use of “Ping-Pong” energy transfer to improve two-photon photodynamic activity of an Ir(III) complex

Zhihui Jin,^{ab} Shuang Qi,^{ab} Xusheng Guo,^{ab} Na Tian,^{ab} Yuanjun Hou,^a Chao Li,^a Xuesong Wang,^{*ab} Qianxiong Zhou^{*a}

^a Key Laboratory of Photochemical Conversion and Optoelectronic Materials, Technical Institute of Physics and Chemistry, Chinese Academy of Sciences, Beijing 100190, P. R. China. Fax: +86-10-62564049; Tel: +86-10-82543592;

^b University of Chinese Academy of Sciences, Beijing 100049, P. R. China.

E-mail: xswang@mail.ipc.ac.cn (X. Wang); zhouqianxiong@mail.ipc.ac.cn (Q. Zhou).

Experimental section

Materials

Pyrenecarboxaldehyde, 2-acetylpyridine, $\text{IrCl}_3 \cdot 3\text{H}_2\text{O}$, 2-phenylpyridine, 2,2':6',2''-terpyridine, 1,3-diphenylisobenzofuran (DPBF), and rhodamine B were purchased from Sigma Aldrich. 30% ammonia solution and sodium hydroxide were purchased from Innochem. DCFH-DA (2,7-dichlorofluorescein diacetate) detection kit and Annexin V-FITC/PI apoptosis detection kit were purchased from Solarbio. Dulbecco's modification of Eagle's medium (DMEM), penicillin, streptomycin, and fetal bovine serum were purchased from Corning.

Instruments

^1H NMR spectra were recorded on a Bruker DMX-400 MHz spectrophotometer. ESI mass spectrometry (ESI-MS) spectra were recorded on a Bruker APEX IV(7.0T) FT_MS. UV-vis absorption spectra were obtained on a Shimadzu UV-1601 spectrophotometer.

An LED lamp (420 ± 10 nm) was used as the light source for one-photon assays. Two-photon absorption cross-sections (δ_2) of the samples were obtained by the two-photon excited fluorescence (TPEF) method with a Ti:sapphire femtosecond laser system (600-2600 nm, 1000 Hz, 25 fs) as the light source.

Nanosecond transient absorption measurements were performed on a LP-980KS laser flash photolysis setup (Edinburgh). Excitation at 405 nm with a power of $2.0 \text{ mJ pulse}^{-1}$ from a computer-controlled Nd:YAG laser/OPO system from Opotek (Spectra Physics) operating at 10 Hz was directed to the sample with an optical absorbance of 0.2 at the excitation wavelength. The laser and analyzing light beam passed perpendicularly through a 1 cm quartz cell. The complete time-resolved spectra were obtained using a gated CCD camera (Andor iSTAR); the kinetic traces were detected by a Tektronix MDO 3022 oscilloscope and a R928P photomultiplier and analyzed by Edinburgh analytical software (LP980KS). All samples used in the flash photolysis experiments were deaerated for 30 min with argon before measurements.

Transient fluorescence spectroscopy were collected on steady state and transient state fluorescence Spectrometer FLS 1000.

Laser confocal scanning microscope images were collected on an Olympus FV1000.

DFT theoretical calculations

All calculations were carried out with the Gaussian 09 (G09) program package 3,^[1] using the density functional theory (DFT) method with Becke's three-parameter hybrid functional and LeeYang-Parr's gradient corrected correlation functional (B3LYP).^[2] The LANL2DZ basis set and effective core potential were used for Ir atom,^[3] and the 6-31 G** basis set was used for other atoms.^[4] The ground-state geometry of the complex was optimized in CH_3CN using the conductive polarizable continuum model (CPCM), and frequency calculation was performed to verify that the optimized structure was in an energy minimum state.

MTT assay

Cells were seeded in 96-well plates at a density of 5000-8000 per well for 24 h. The medium containing different concentrations of drugs was added into each well. After incubation for 4 h, the medium was changed. Light groups were illuminated with a 420 nm (22.5 mW/cm^2) LED lamp for 30 min and then incubated for another 20 h. Cell medium was discarded and MTT (3-(4,5-dimethyl-2-thiazolyl)-2,5-diphenyl tetrazolium bromide) (1 mg/mL) was added. After 4 h the solution was discarded and DMSO was added. The data was obtained by a Thermo MK3

Multiscanmicroplate reader at 570nm.

Apoptosis staining assay

Annexin V-FITC and PI are double staining reagents for detecting apoptosis and necrosis. SKOV-3 cells were cultured with different concentrations of complexes **1** and **2** for 4 h. The light group was irradiated with a 420 nm (22.5 mW/cm²) LED lamp for 30 min, and then placed in an incubator for 10 h. The cells were trypsinized, centrifuged and washed 3 times with PBS, stained with Annexin V-FITC and PI, then detected by flow cytometry.

Apoptosis imaging by confocal microscopy

SKOV-3 cells were co-cultured with medium containing 2 nM complex **1** for 4 h, then the medium was changed. The light group was irradiated with a 420 nm (22.5 mW/cm²) LED lamp for 30 min, then placed in an incubator for 10 h. The medium was refreshed with that containing Annexin V-FITC and PI. After 20 min, the cells were washed for three times with PBS and analyzed using confocal microscopy (excited at 488 nm).

Fluorescence quantum yield measurement

Fluorescence quantum yield of 4-(pyren-1-yl)-tpy (tpy-py) was measured according to a reported method.^[5] Quinine sulfate was used as the reference. The calculation formula was given as below,

$$\varphi_f = \varphi_{fR} \times \frac{I}{I_R} \times \frac{A_R}{A} \times \frac{n^2}{n_R^2}$$

in which φ_f stands for fluorescence quantum yield, I stands for the integrated emission intensity, n stands for the refractive index, A stands for the absorbance at excitation wavelength, and the subscript of R stands for reference.

Two-Photon absorption cross section measurements

Two-photon absorption cross sections of tpy-py were measured according to a reported method with Rhodamine B as the reference,^[6] and calculated as follows.

$$\delta_2^2 = \frac{F_2}{F_1} \cdot \frac{\varphi_{f1}}{\varphi_{f2}} \cdot \frac{n_1}{n_2} \delta_2^1$$

δ_2 stands for two-photon absorption cross section; F stands for integral area of fluorescence spectrum; φ_f stands for fluorescence quantum yield; n stands for the concentration of the sample. The numbers of 1 and 2 stand for the reference and sample, respectively.

Singlet oxygen quantum yield measurement

The measurement of singlet oxygen quantum yield (Φ) was carried out according to a reported method,^[7] using 1,3-diphenylisobenzofuran as the singlet oxygen capture agent and [Ru(bpy)₃]²⁺ ($\Phi = 0.81$ in CH₃OH) as the reference. The sample was irradiated with 440 nm light in a Hitachi F-4600 fluorescence spectrophotometer (slit width: 10 nm). The relative singlet oxygen quantum yield was calculated by the following formulas:

$$\frac{-\Delta[DPBF]}{t} = \frac{I_0 - I_t}{t} = I_{in} \Phi_{ab} \Phi_{\gamma} \Phi_{\Delta}$$

$$\frac{k}{k_S} = \frac{\Phi_{ab} \Phi_{\gamma} \Phi_{\Delta}}{\Phi_{ab}^S \Phi_{\gamma}^S \Phi_{\Delta}^S}$$

in which t stands for irradiation time; Φ_{ab} , Φ_{γ} , Φ_{Δ} stand for the light absorption efficiency of the photosensitizer, the reaction efficiency of DPBF and ¹O₂, and the singlet oxygen quantum yield,

respectively; I_{in} , I_0 and I_t are incident light intensity, DPBF fluorescence intensity before illumination and DPBF fluorescence intensity after illumination, respectively.

Cell morphological change upon two-photon irradiation

SKOV-3 cells were cultured with medium containing complexes **1** or **2** (0.2 μ M) for 4 h. Then medium was discarded and the cells were washed with PBS three times. The cells were illuminated with femtosecond laser (740 nm, 12.7 W/cm²) equipped in the confocal microscope, the morphological changes of which were imaged.

Confocal imaging of intracellular singlet oxygen generation

SKOV-3 cells were cultured with medium containing complexes **1** or **2** (0.2 μ M) for 4 h. After changing the medium, the cells were cultured with DCFH-DA (2,7-dichlorofluorescein diacetate) for 20 min. Then the medium was discarded and the cells were washed with PBS three times. The light groups were irradiated in either one-photon (403 nm) or two-photon (740 nm femtosecond laser) mode. Confocal luminescence images were recorded by monitoring the green channel at 490-520 nm.

Cytotoxicity on 3D multicellular spheroids (MCSs)

5000 ~ 8000 SKOV-3 cells were seeded in a 96-well plate to form MCSs with diameters of about 400 μ m. Complexes **1** or **2** (0.2 μ M) was added and co-cultured with MCSs for 8 h. Then the solution was refreshed. The light group was irradiated with 800 nm (1 W/cm²) for 20 min, and incubated for another 24 h, then stained with Calcein AM and PI. Images were recorded by confocal microscope.

Synthesis and characterization of the tpy-py ligand^[8]

To a solution of 1-pyrenecarboxaldehyde (2.42 g, 21 mmol) in ethanol (60 ml) was added 2-acetylpyridine (4.8 g, 40 mmol), sodium hydroxide (1.6 g, 40 mmol) and aqueous ammonia (60 mL, 30%). The reaction mixture kept at 35 °C for 24 h. After cooling to 25 °C, the solid was filtered and washed with ethanol (30 mL). Recrystallization from ethanol afforded yellow crystalline solid. ¹H NMR (400 MHz, Chloroform-*d*) δ 7.32-7.40 (ddd, J = 7.4, 4.8, 1.3 Hz, 2H), 7.88-7.96 (td, J = 7.7, 1.7 Hz, 2H), 7.99-8.09 (m, 2H), 8.10-8.15 (m, 3H), 8.16-8.30 (m, 4H), 8.67-8.72 (d, J = 4.8 Hz, 2H), 8.73-8.81 (m, 4H). HR ESI-MS: calculated for (M + H⁺) 434.1657, found: 434.1630.

Synthesis of dichlorotetrakis(2-(2-pyridinyl)phenyl)diiridium(III)

Dichlorotetrakis(2-(2-pyridinyl)phenyl)diiridium(III) was synthesized by the reported methods.^[9]

Synthesis and characterization of [Ir(ppy)₂(tpy-py)]⁺(1)^[9]

100 mg dichlorotetrakis(2-(2-pyridinyl)phenyl)diiridium(III) (0.0933 mmol) and 89 mg tpy-py (0.207 mmol) were refluxed (150 °C) in ethylene glycol under an argon atmosphere for 15 h. After cooling to room temperature, cyclohexane and water were added, and most of the ethylene glycol was washed away with separating funnel. The target compound was precipitated with NH₄PF₆, then was filtered and washed with diethyl ether and dried to give an orange solid. The orange solid was recrystallized from acetone/water to yield the pure product (Yield: 73%). HPLC purity > 95%. ¹H NMR (400 MHz, CD₃CN) δ 5.43-5.52 (d, J = 7.6 Hz, 1H), 5.89-5.96 (d, J = 7.7 Hz, 1H), 6.18-6.25 (t, J = 7.4 Hz, 1H), 6.47-6.54 (t, J = 7.5 Hz, 1H), 6.63-6.70 (t, J = 7.4 Hz, 1H), 6.82-6.89 (t, J = 6.4 Hz, 2H), 6.90-6.97 (m, 1H), 7.11-7.21 (t, J = 6.8 Hz, 2H), 7.26-7.33 (t, J = 6.5 Hz, 1H), 7.38-7.45 (d, J = 7.8 Hz, 1H), 7.53-7.60 (m, 1H), 7.70-7.75 (d, J = 7.7 Hz, 1H), 7.79-7.87 (q, J = 6.3, 5.8 Hz, 3H), 7.88-8.01 (dt, J = 17.6, 8.5 Hz, 3H), 8.01-8.09 (t, J = 8.8 Hz, 2H),

8.10-8.29 (m, 8H), 8.29-8.39 (dd, $J = 14.2, 7.8$ Hz, 2H), 8.88-8.95 (d, $J = 8.1$ Hz, 1H), 8.97-9.04 (s, 1H), 9.24-9.32 (d, $J = 4.7$ Hz, 1H). HR ESI-MS: calculated m/z for $(M - PF_6^-)^+$: 934.2522, found: 934.2529.

Synthesis and characterization of $[Ir-(ppy)_2(tpy)]^+(2)$

Complex **2** was synthesized with a procedure similar to that of **1**. HPLC purity >95%. 1H NMR (400 MHz, CD_3CN) δ 5.43-5.49 (d, $J = 7.6$ Hz, 1H), 5.88-5.94 (d, $J = 7.7$ Hz, 1H), 6.29-6.37 (t, $J = 7.5$ Hz, 1H), 6.57-6.70 (m, 2H), 6.74-6.82 (t, $J = 7.6$ Hz, 1H), 6.91-7.05 (m, 3H), 7.13-7.25 (dt, $J = 18.6, 7.2$ Hz, 2H), 7.37-7.52 (m, 3H), 7.54-7.59 (d, $J = 5.9$ Hz, 1H), 7.69-7.74 (d, $J = 7.8$ Hz, 1H), 7.76-7.82 (d, $J = 5.5$ Hz, 1H), 7.83-7.99 (m, 3H), 8.00-8.06 (d, $J = 8.3$ Hz, 1H), 8.15-8.26 (m, 3H), 8.58-8.64 (d, $J = 8.2$ Hz, 2H), 8.78-8.89 (s, 1H). HR ESI-MS: calculated m/z for $(M - PF_6^-)^+$: 734.1896, found: 734.1880.

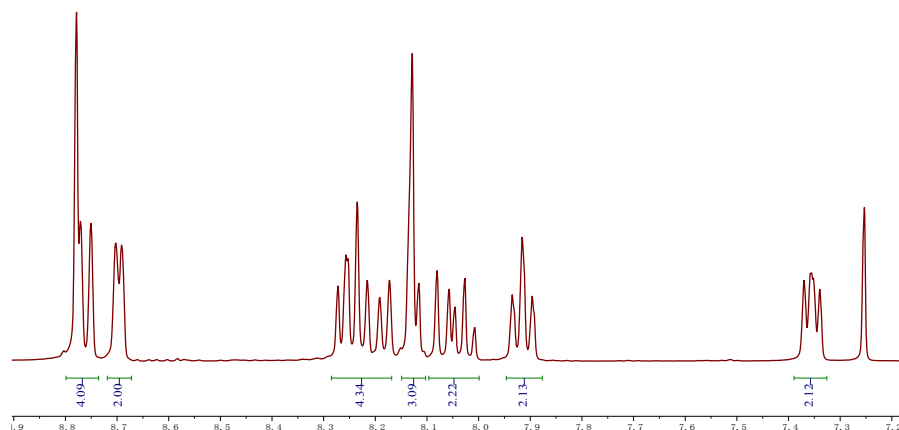


Fig. S1 1H NMR spectrum of tpy-py in chloroform-*d*.

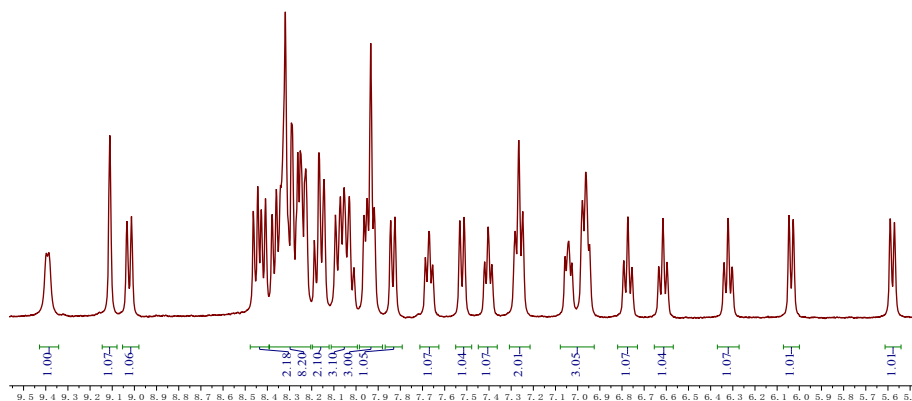


Fig. S2 ^1H NMR spectrum of **1** in CD_3CN .

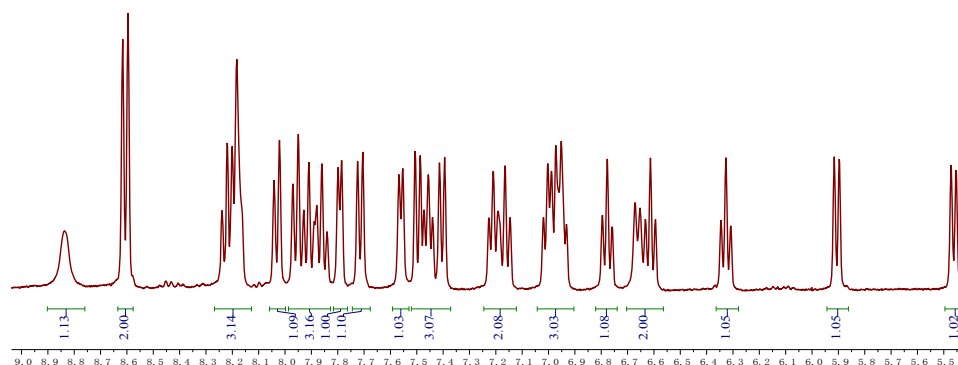


Fig. S3 ^1H NMR spectrum of **2** in CD_3CN .

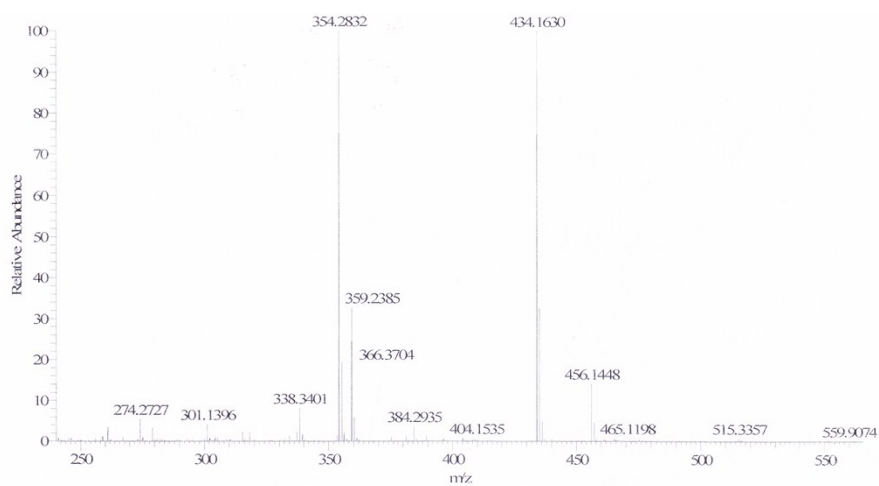


Fig. S4 ESI mass spectrum of tpy-py.

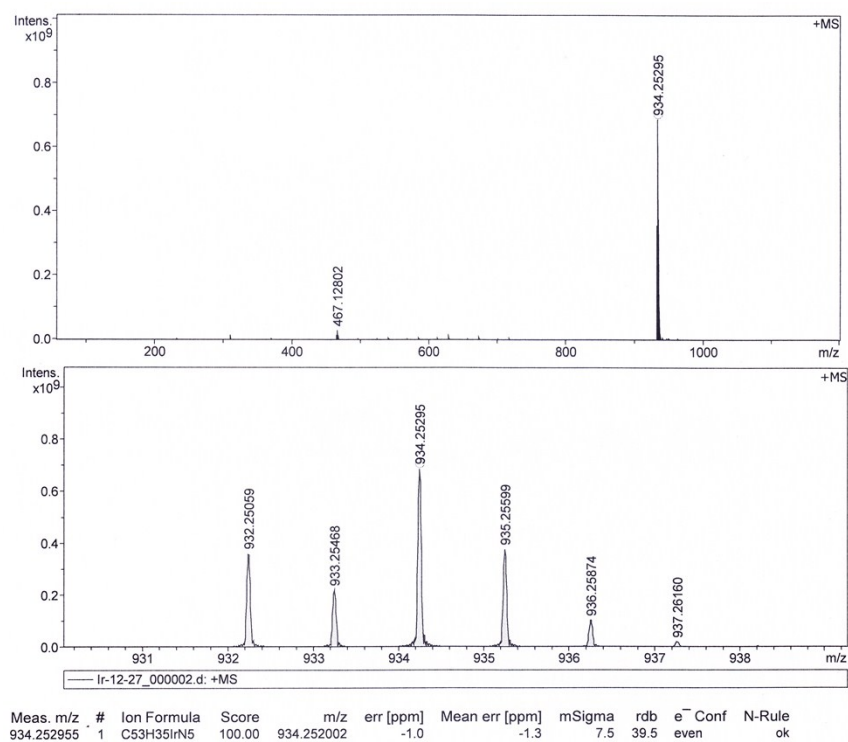


Fig. S5 ESI mass spectra of complex 1.

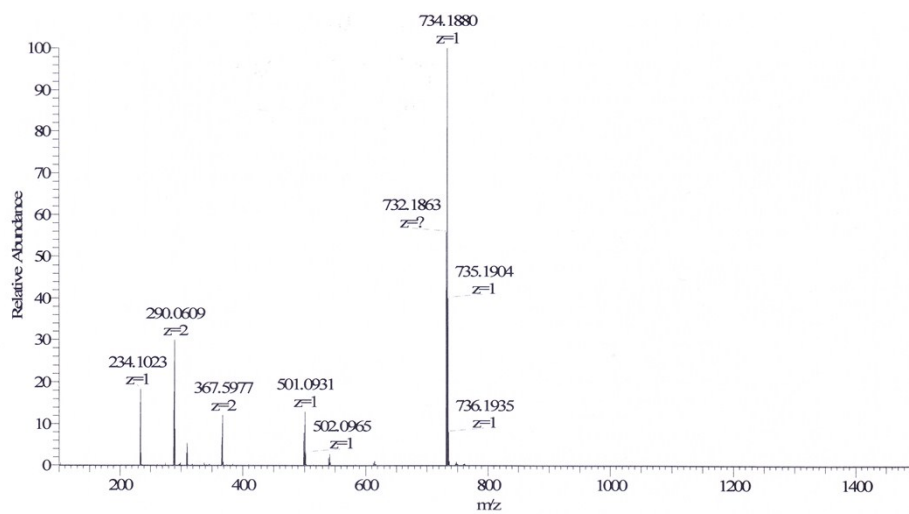


Fig. S6 ESI mass spectrum of complex 2.

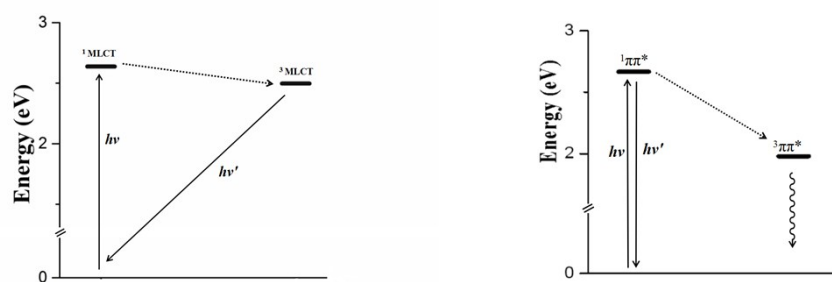


Fig. S7 Energy level diagrams of complex **1** (left) and the tpy-py ligand (right) based on the calculated results.

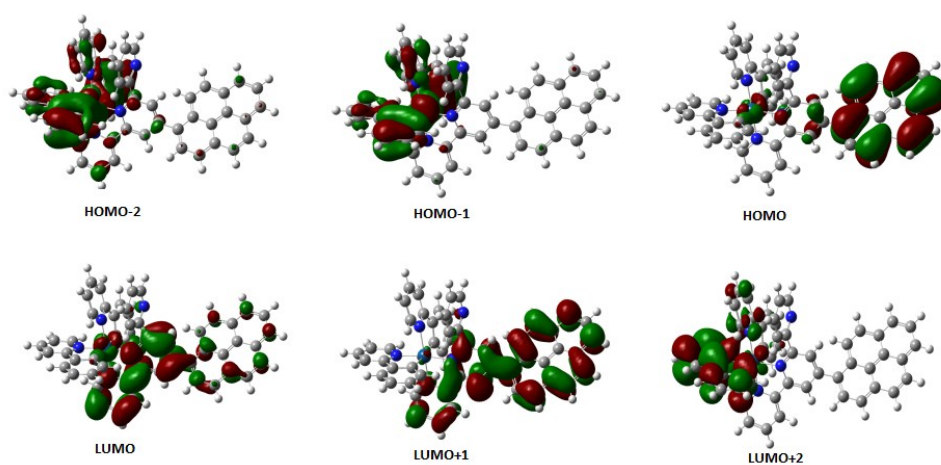


Fig. S8 Selected orbitals of complex **1**.

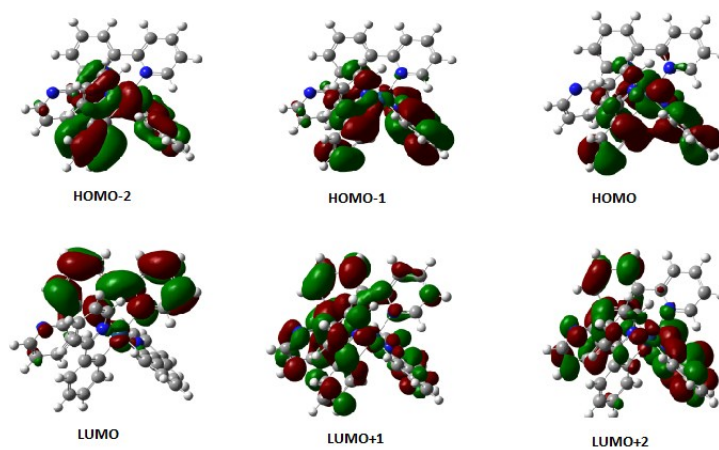


Fig. S9 Selected orbitals of complex **2**.

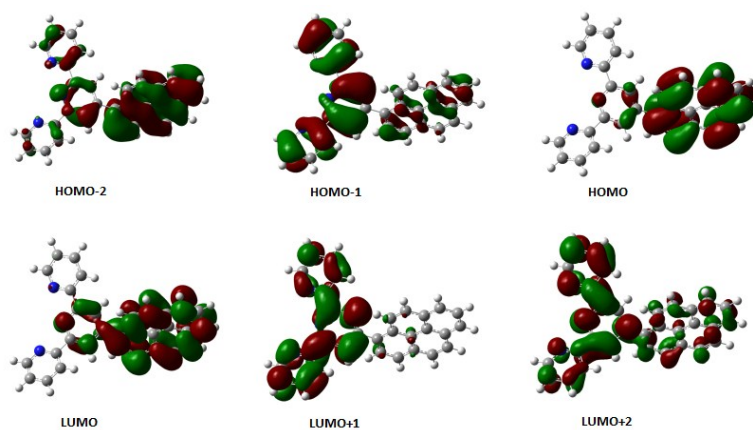


Fig. S10 Selected orbitals of tpy-py.

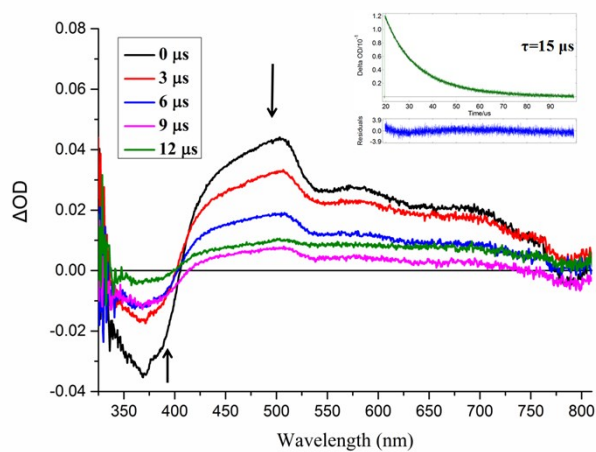


Fig. S11 Transient absorption spectra of complex **1** in degassed CH_3CN upon excitation by 405 nm of pulsed laser. Inset is the transient absorption decay at 510 nm.

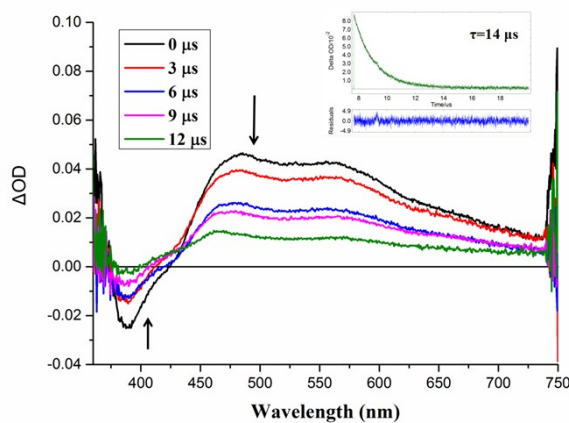


Fig. S12 Transient absorption spectra of tpy-py in degassed CH_3CN upon excitation by 405 nm of pulsed laser. Inset is the transient absorption decay at 510 nm.

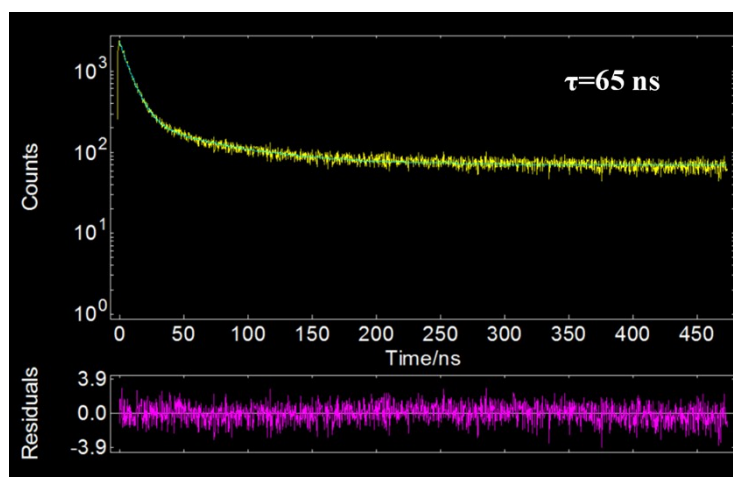


Fig. S13 Time-resolved luminescent decay of complex **2** in degassed CH₃CN.

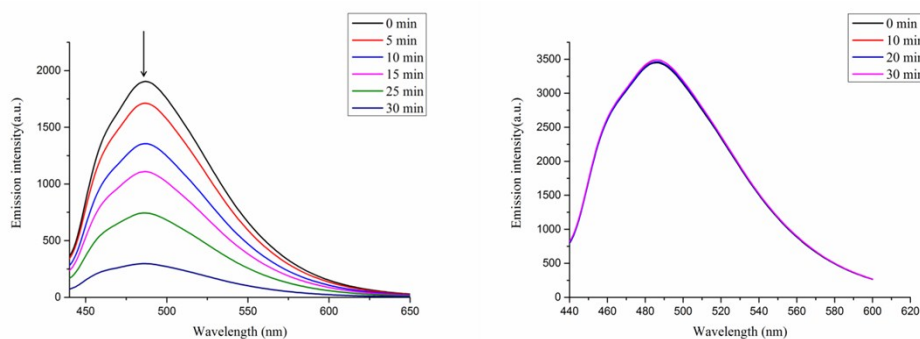


Fig. S14 Emission spectra changes of the CH₃CN solutions containing 1,3-diphenylisobenzofuran (DPBF, 10 μM) and **1** (20 μM, left) or **2** (20 μM, right) under two-photon femtosecond laser (800 nm, 1000 Hz, 1 W/cm²) irradiation.

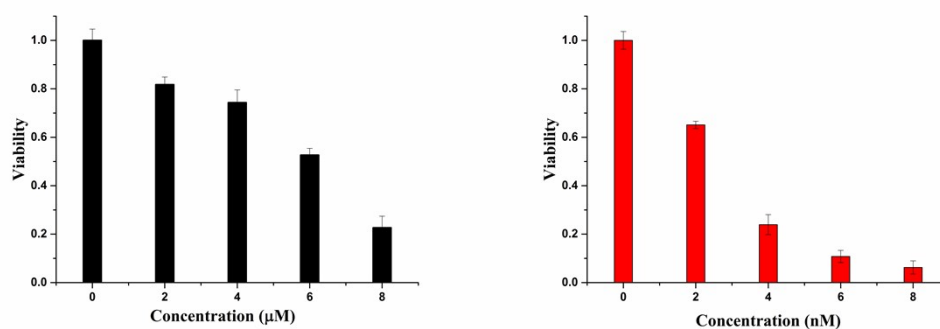


Fig. S15 Cytotoxicity of **1** towards SKOV-3 cells in the dark (left) or upon irradiation (right) with a 420 nm LED lamp for 30 min (22.5 mW/cm²).

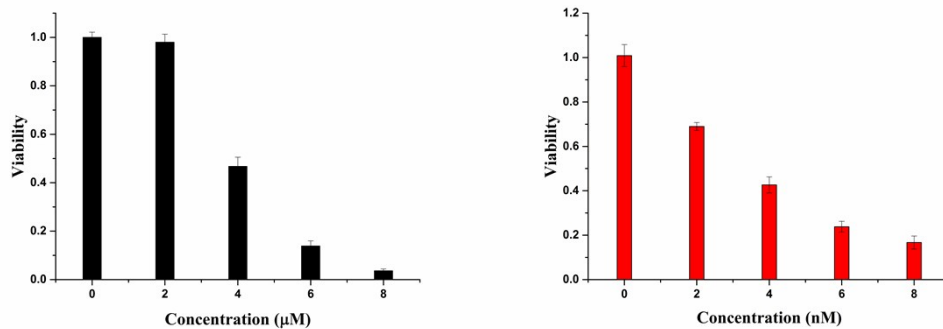


Fig. S16 Cytotoxicity of **1** towards A549 cells in the dark (left) or upon irradiation (right) with a 420 nm LED lamp for 30 min (22.5 mW/cm²).

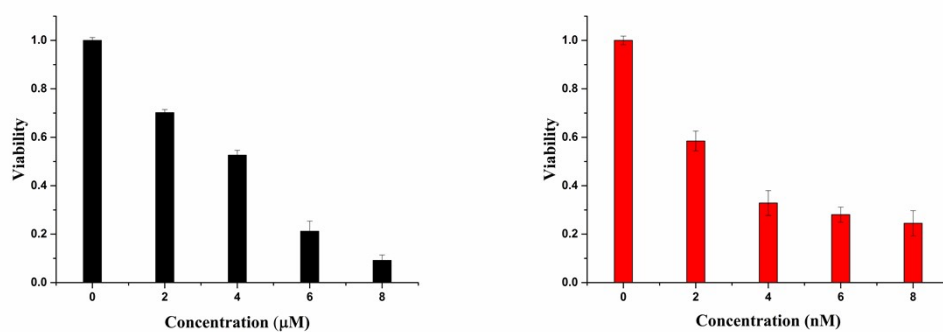


Fig. S17 Cytotoxicity of **1** towards L-02 cells in the dark (left) or upon irradiation (right) with a 420 nm LED lamp for 30 min (22.5 mW/cm²).

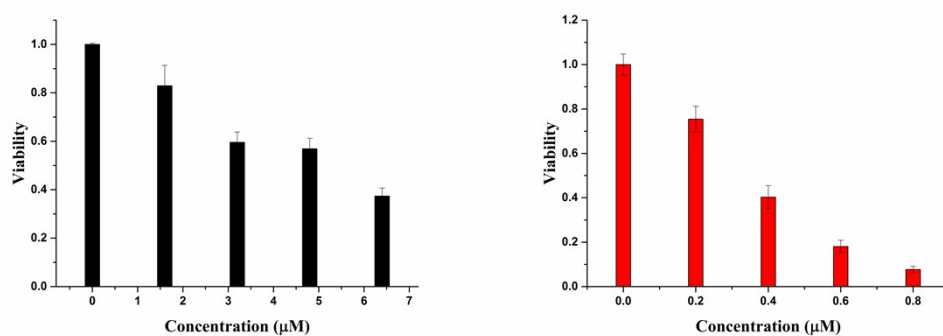


Fig. S18 Cytotoxicity of **2** towards SKOV-3 cells in the dark (left) or upon irradiation (right) with a 420 nm LED lamp for 30 min (22.5 mW/cm²).

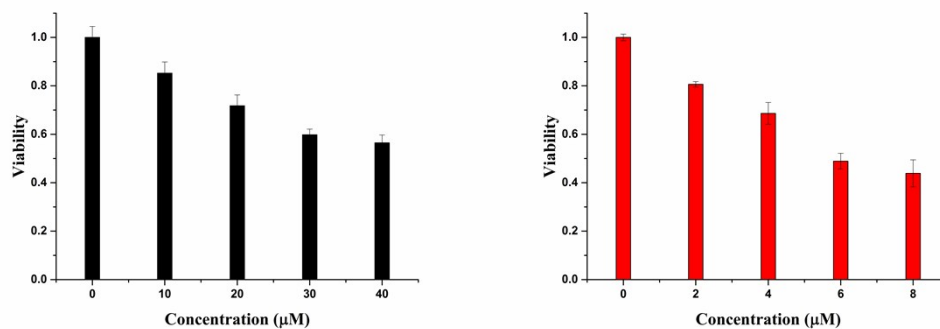


Fig. S19 Cytotoxicity of **2** towards A549 cells in the dark (left) or upon irradiation (right) with a 420 nm LED lamp for 30 min (22.5 mW/cm²).

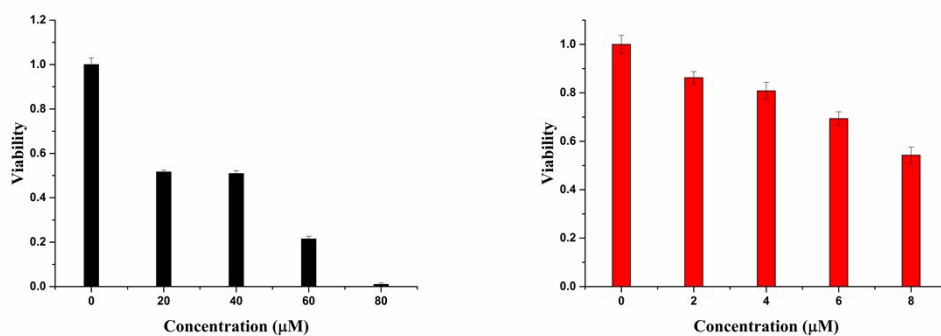


Fig. S20 Cytotoxicity of **2** towards L-02 cells in the dark (left) or upon irradiation (right) with a 420 nm LED lamp for 30 min (22.5 mW/cm²).

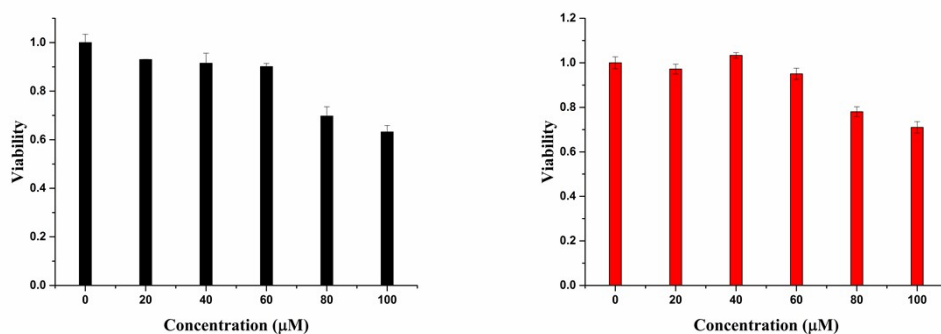


Fig. S21 Cytotoxicity of **cisplatin** towards SKOV-3 cells in the dark (left) or upon irradiation (right) with a 420 nm LED lamp for 30 min (22.5 mW/cm²).

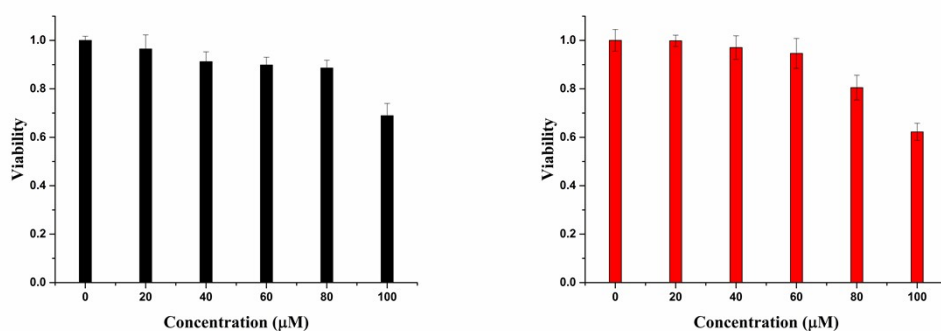


Fig. S22 Cytotoxicity of **cisplatin** towards A549 cells in the dark (left) or upon irradiation (right) with a 420 nm LED lamp for 30 min (22.5 mW/cm²).

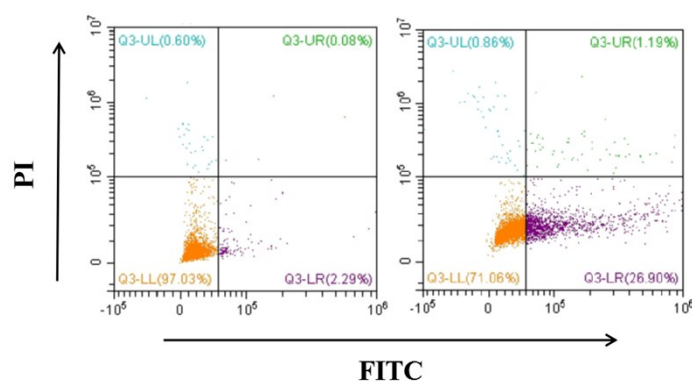


Fig. S23 Flow-cytometric analysis of SKOV-3 cells based on Annexin V-FITC and PI staining. The cells were treated with complex **1** (2 nM) in the dark (left) or irradiated for 30 min with 420 nm (22.5 mW/cm²) LED light.

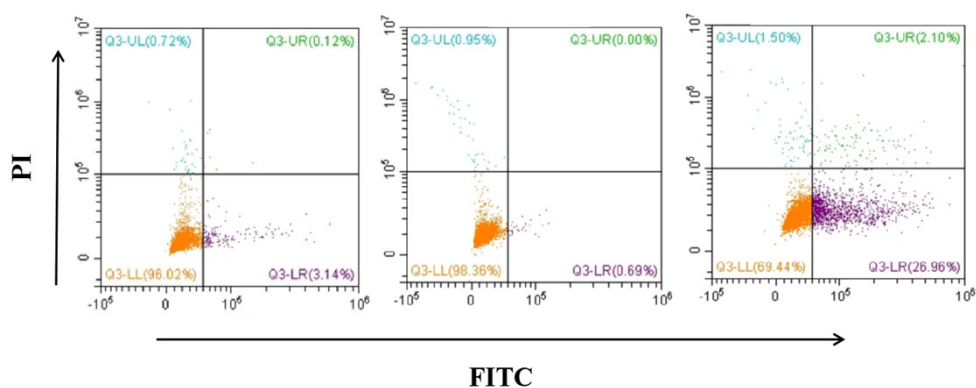


Fig. S24 Flow-cytometric analysis of SKOV-3 cells based on Annexin V-FITC and PI staining. The cells were treated with only light (left), or with complex **2** (3 μ M) in the dark (middle), or with **2** and irradiation for 30 min with 420 nm (22.5 mW/cm²) LED light.

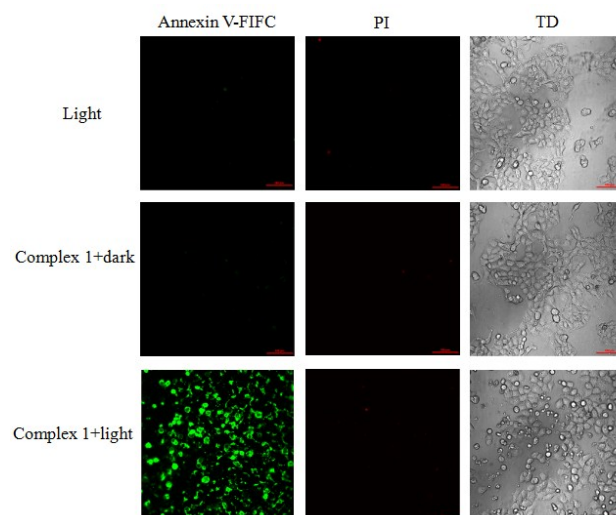


Fig. S25 Confocal luminescence images of Annexin V-FITC/PI stained SKOV-3 cells after treatment with complex **1** (2 nM) in the dark or irradiated for 30 min with 420 nm (22.5 mW/cm²) LED light. Scale bars: 100 μ m.

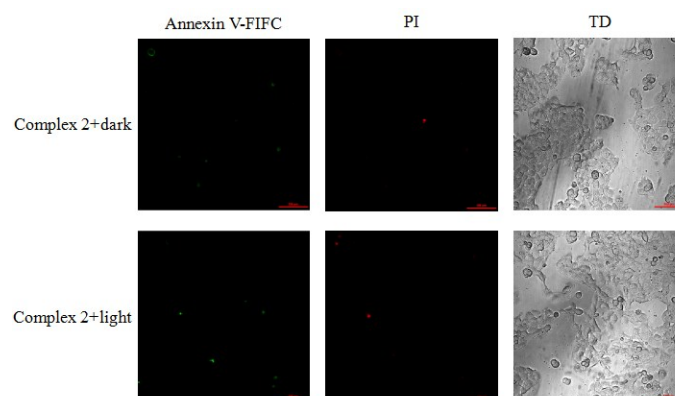


Fig. S26 Confocal luminescence images of Annexin V-FITC/PI stained SKOV-3 cells after treatment with complex **2** (2 nM) in the dark or irradiated for 30 min with 420 nm (22.5 mW/cm²) LED light. Scale bars: 100 μ m.

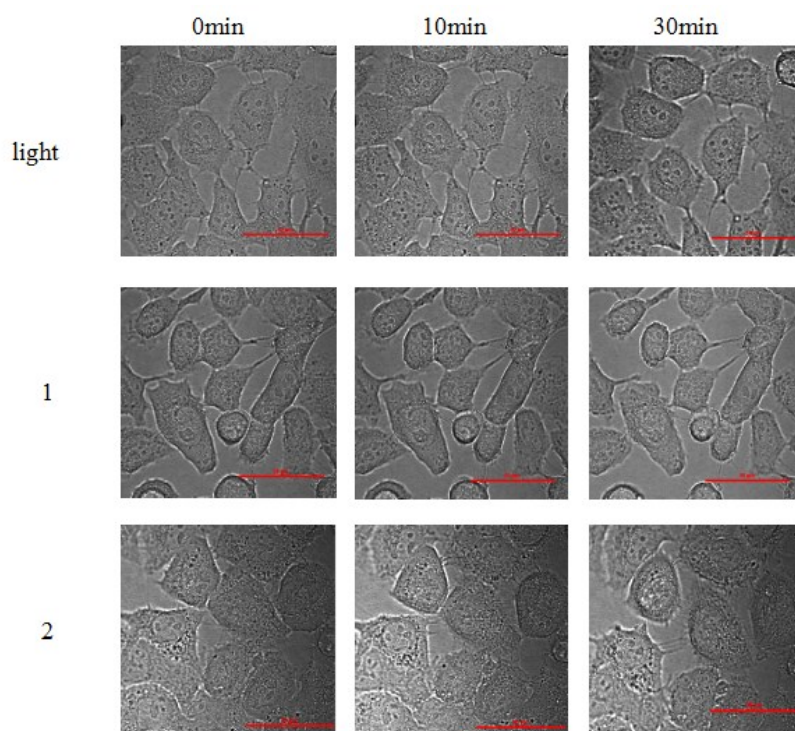


Fig. S27 Confocal images of SKOV-3 cells treated only with femtosecond laser (740 nm, 1 W/cm²) or with complexes **1-2** (0.2 μM) in the dark. Scale bars: 50 μm.

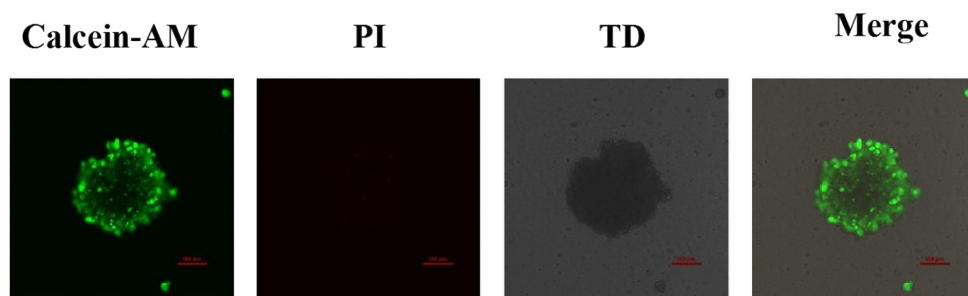


Fig. S28 The images of an SKOV-3 MCS stained by Calcein AM and PI and treated only by two-photon irradiation (800 nm, 1W/cm²). Scale bars: 100 μm.

Table S1. SKOV-3 uptake levels of **1-2**.

	1	2
pmol/10 ⁶ cell ^a	4.61 ± 0.24	26.4 ± 2.2

^a Measured by Ir content using inductively coupled plasma mass spectrometry (ICP-MS)

Table S2. Three minimum singlet state transitions of complex **1** based on TD-DFT calculation (H = HOMO, L = LUMO).

Singlet Excited state	Energy (eV)	Wavelength (nm)	Oscillator Strength (f)	Calculated transitions and Orbital contributions
1	2.5762	481.26	0.1535	H-1 → L(36%) H → L (61%)
2	2.6660	465.06	0.1152	H-1 → L(60%) H → L(36%)
3	2.9157	425.23	0.0484	H-2 → L(94%)

Table S3. Three minimum triplet state transitions of complex **1** based on TD-DFT calculation (H = HOMO, L = LUMO).

Triplet Excited state	Energy (eV)	Wavelength (nm)	Oscillator Strength (f)	Calculated transitions and Orbital contributions
1	1.9796	626.30	0.0000	H → L (35%) H → L+1 (47%) H → L+5 (5%)
2	2.4815	499.63	0.0000	H-2 → L (5%) H-1 → L (48%) H → L (22%) H → L+1 (9%)
3	2.5772	481.09	0.0000	H-2 → L (37%) H-1 → L (29%) H → L (12%) H → L+1 (5%)

Table S4. Three minimum singlet state transitions of complex **2** based on TD-DFT calculation (H = HOMO, L = LUMO).

Singlet excited state	Energy (eV)	Wavelength (nm)	Oscillator Strength (f)	Calculated transitions and Orbital contributions
1	2.6369	470.19	0.0009	H → L (98%)
2	3.1084	398.87	0.0382	H → L+1 (38%) H → L+2 (58%)
3	3.2046	386.90	0.0031	H → L+1 (41%) H → L+2 (32%) H → L+3 (24%)

Table S5. Three minimum triplet state transitions of complex **2** based on TD-DFT calculation (H = HOMO, L = LUMO).

Triplet excited state	Energy (eV)	Wavelength (nm)	Oscillator Strength (f)	Calculated transitions and Orbital contributions
1	2.2966	496.60	0.0000	H → L (93%)
2	2.8101	441.21	0.0000	H-1 → L+3 (7%) H → L+1 (15%) H → L+2 (37%) H → L+3 (15%)
3	2.8483	435.30	0.0000	H-1 → L+2 (21%) H → L+1 (5%) H → L+2 (21%) H → L+3 (30%)

Table S6. Three minimum singlet state transitions of tpy-py based on TD-DFT calculation (H = HOMO, L = LUMO).

Singlet excited state	Energy (eV)	Wavelength (nm)	Oscillator Strength (f)	Calculated transitions and Orbital contributions
1	3.3130	374.23	0.5265	H → L (92%) H → L+2 (5%)
2	3.5927	345.10	0.0033	H → L+2 (92%)
3	3.6966	335.40	0.0297	H-1 → L (37%) H → L+2 (18%) H → L+3 (34%)

Table S7. Three minimum triplet state transitions of tpy-py based on TD-DFT calculation (H = HOMO, L = LUMO).

Triplet excited state	Energy (eV)	Wavelength (nm)	Oscillator Strength (f)	Calculated transitions and Orbital contributions
1	2.0536	603.73	0.0000	H → L (85%) H → L+2 (9%)
2	3.1634	391.94	0.0000	H-6 → L+2 (7%) H-2 → L+1 (45%) H-1 → L+1 (5%) H → L+2 (10%)
3	3.3654	368.40	0.0000	H-2 → L+1 (9%) H-1 → L (25%) H → L+1 (9%) H → L+2 (12%) H → L+3 (30%)

References

1. R. D. Gaussian 09, G. W. T. M. J. Frisch, H. B. Schlegel, G. E. Scuseria, J. R. C. M. A. Robb, G. Scalmani, V. Barone, B. Mennucci, H. N. G. A. Petersson, M. Caricato, X. Li, H. P. Hratchian, J. B. A. F. Izmaylov, G. Zheng, J. L. Sonnenberg, M. Hada, K. T. M. Ehara, R. Fukuda, J. Hasegawa, M. Ishida, T. Nakajima, O. K. Y. Honda, H. Nakai, T. Vreven, J. A. Montgomery, Jr., F. O. J. E. Peralta, M. Bearpark, J. J. Heyd, E. Brothers, V. N. S. K. N. Kudin, T. Keith, R. Kobayashi, J. Normand, A. R. K. Raghavachari, J. C. Burant, S. S. Iyengar, J. Tomasi, N. R. M. Cossi, J. M. Millam, M. Klene, J. E. Knox, J. B. Cross, C. A. V. Bakken, J. Jaramillo, R. Gomperts, R. E. Stratmann, A. J. A. O. Yazyev, R. Cammi, C. Pomelli, J. W. Ochterski, K. M. R. L. Martin, V. G. Zakrzewski, G. A. Voth, J. J. D. P. Salvador, S. Dapprich, A. D. Daniels, J. B. F. O. Farkas, J. V. Ortiz, J. Cioslowski, G. and D. J. Fox, Gaussian 09, Gaussian, Inc., Wallingford CT, 2013.
2. (a) A. D. Becke, *J. Chem. Phys.*, 1993, **98**, 5648-5652; (b) C. Lee, W. Yang, R. G. Parr, *Phys Rev B Condens Matter*, 1988, **37**, 785-789.
3. P. J. H. a. R. L. M. L. E. Roy, *J. Chem. Theory Comput.*, 2008, **4**, 1029-1031.
4. (a) W. M. M. Francl, W. J. H. J. Pietro, J. S. Binkley, M. S. Gordon, D. J. Defrees and J. A. Pople, *J. Chem. Phys.*, 1982, **77**, 3654-3665; (b) P. C. Hariharan and J. A. Pople, *Theor. Chim. Acta*, 1973, **28**, 213-222.
5. L. He, M. Fei, J. Chen, Y. Tian, Y. Jiang, Y. Huang, K. Xu, J. Hu, Z. Zhao, Q. Zhang, H. Ni, L. Chen, *Mater. Today*, 2019, **22**, 76-84.
6. C. Xu, W. W. Webb, *J. Opt. Soc. Am. B: Opt. Phys.*, 1996, **13**, 481-491.
7. P. D. B. Ayman A. Abdel-Shafi, Roger J. Mortimer, and Francis Wilkinson, *J. Phys. Chem.*, 2000, **104**, 192-202.
8. R. Joseph, A. Nkrumah, R. J. Clark, E. Masson, *J. Am. Chem. Soc.*, 2014, **136**, 6602-6607.
9. M. S. Lowry, W. R. Hudson, R. A. Pascal, B. Stefan, *J. Am. Chem. Soc.*, 2004, **126**, 14129-14135.